Characterization of an in situ chamber for catalytic studies using LIF

Bachelor Thesis, 15 hp

Jonas Evertsson

Supervisor:

Johan Gustafson

Division of Synchrotron Radiation Research

Department of Physics

LUND UNIVERSITY

Contents

1 Acknowledgements

First of all I would like to thank my supervisor, Johan Gustafson, who helped me a lot with both the content and the text in the work. I am very grateful for everything I have learned and it was a very nice experience to do the project with Johan as my supervisor.

For the text correction, I would also like to thank Carl-Erik Magnusson, who corrected the initial versions.

I would also like to thank Sara Blomberg, Edvin Lundgren, and Johan Zetterberg for their help during and after the experiments.

Finally, I would like to thank the Division of Synchrotron Radiation Research for letting me write my thesis there, along with the people there for the nice coffee breaks.

2 Populärvetenskaplig sammanfattning - Katalyskammare för aktivitetsmätning med laser (Swedish)

Katalysatorer är mycket viktiga för den industrialiserade delen av världen. Ett tydligt exempel är bensindrivna bilar där katalysatorer används till både bränsletillverkningen och avgasreningen. I och med att världen blir mer industrialiserad måste mycket förbättras, katalysatorer inräknat. I mitt examensarbete har jag karakteriserat en ny typ av reaktorkammare där Laser Inducerad Flourescens (LIF) används för aktivitetsmätning av katalysatorer.

Industriella katalysatorer för CO och CH_4 oxidering är mycket komplexa system ofta bestående av katalytiskt aktiva nanopartiklar utspridda i ett supportmaterial. Dessa katalysatorer är mycket svåra att undersöka med ytfysikens metoder. Därför har det under många år använts modeller med enkla kristallprover, ultra högt vakuum och ex situ metoder, vilka långt ifrån avspeglar industriella katalysatorer.

Men under senare år har nya *in situ* tekniker utvecklats som möjliggör mer realistiska modeller och därför har förståelsen ökat. I mitt projekt har jag karakteriserat ett experimentsystem med en ny typ av reaktorkammare för *in situ* analys av katalysatorer. Med kammaren ska CO_2 producerat från CO- och CH_4-oxidering med hjälp av katalysatorer mätas med en laser (LIF), vilket möjliggör jämförelse av flera olika prover samtidigt i kammaren.

Systemet kan användas till både flödesexperiment och stängda experiment för tryck mellan 10^{-2} och 1000 mbar, men den stora kammaren, 200 ml, gör den mest lämpad för det senare. Förutom LIF mätning av CO_2 är andra gaser mätbara med en masspektrometer.

Det gjordes också två reaktionsmätningar med systemet. I det första jämfördes CO oxidering på Pd(100) och PdAg(100) för att se om Pd atomerna i legeringen segregerar till ytan och ger samma aktivitet som det rena Pd provet. Försöket visade att aktivitet för PdAg nådde samma nivå eller nästan samma nivå som Pd provet, men efter längre tid, troligtvis på grund av att Pd atomerna behöver segregera upp till ytan av provet.

I det andra experimentet användes LIF för att jämföra reaktiviteten för två mycket reaktiva pulverprover. I samma experiment syntes det vid låga temperaturer att ett prov med 1 % Pd och 2 % Pt i ett Aluminiumoxidpulver var mer reaktivt än ett liknande prov med 4 % Pd.

Under försöket syntes mycket tydligt tre aktivitetsfaser och skillnaden för faserna mellan de olika proverna i reaktorn. Slutsatsen är att systemet fungerade bra och genom att förbättra noggrannheten kommer det i framtiden troligtvis vara användbart.

3 Abstract

Industrial catalysts are very complex systems, often produced of nanoparticles dispersed in a so-called support material to maximize the surface area and minimize the cost. These catalysts are very difficult to study in surface science. Therefore industrial catalysts have been developed in a trial-and-error approach, with the loss of the fundamental understanding of the reactions.

In surface science, CO and CH_4 oxidation have been studied for many years in model systems using single crystal samples, ultra high vacuum and *ex situ* techniques, which means that many of the properties of real industrial catalysts will be lost. For a few years, better *in situ* methods operating in higher vacuum have been developed to get closer to the real systems.

In this project I have characterized a new type of *in situ* system with both industrial and surface science applications. The idea is that the CO_2, produced in an oxidation reaction, should be measured with Laser-Induced Fluorescence (LIF), directly giving a spatially resolved image of the CO_2 produced over each of several samples in the reactor. This makes it possible to compare different catalysts in a live mode.

The system can be used for both flow and batch experiments for pressures between 10^2 - 1000 mbar, but the rather large reactor, 200 ml, makes it best suited for the later. In addition to the LIF measured CO_2, also other gases are measurable with a Quadrupole Mass Spectrometer. The sample temperature is controlled by a bohr electric heater and measured with a thermocouple.

Performance and some catalysis measurements were used to characterize the system and find possible improvements. In a test experiment using LIF the results were good. Together with some improvements the next measurement could give more accurate results, making it possible to compare different catalytic samples.

In this thesis two measurements are presented. The first compares CO oxidation on Pd(100) and PdAg(100) to see if the Pd atoms can segregate to the surface of the alloy and give the same activity as the pure Pd sample. The result showed that the activity of the PdAg reached the same or almost the same level as the Pd sample, but after longer time probably due to the time it took for the Pd atoms to segregate to the surface.

The second experiment was on two very reactive Powder samples where also LIF was used. In the same experiment it was found that the sample with 1 % Pd + 2 % Pt was more reactive then the 4 % Pd, at least at low temperatures. Three different activity phases of the samples were very clearly seen in the LIF signal. Also the exothermic effect of the CO oxidation, which is an interesting property, could easily be seen in the experiment.

4 Introduction

Catalysis is one of the most important techniques in the industrial part of the world. Different catalysis techniques are for example used both in the fabrication of the fuel used and the cleaning of pollutants from the exhaust in cars. Without catalysis it would be very hard for the industrialization and the environment would have been dangerous. In the future when more and more people in the world want to get the same opportunities as the people in the rich parts the pressure on the environment will increase enormously. To be able to keep this pressure under control many things must be developed and one of these is of course the catalysis techniques.

The catalyst in car engines and other exhaust systems are so-called heterogeneous catalysts, where the gases react with a solid surface. These catalysts have been developed in a trial-and-error kind of method, where simply the best of many almost randomly mixed catalysts have been selected. This is a very fast and cheap way to find a good catalyst but with almost no understanding of what are the important reasons. In surface science one tries to get an understanding with the aim that the industrial developments should turn to the basic science for further developing. This could maybe give a jump in the development as has seen to be the result of many other discoveries of basic science, and in the long run produce better and cheaper catalysis techniques.

The standard techniques used by surface scientists involve either single crystal surface samples, low pressures or even both. This is not as the industrial catalysts, which have many different facets and defects, and are working in atmospheric pressures. The difference between the basic science model catalysts and the industrial catalysts is referred as the Materials Gap and the Pressure Gap. By using many different models that go from more industrial to surface science friendly, the gaps can be reduced and hopefully give a better understanding of the industrial catalysts.

In this project I have characterized a new type of *in situ* reactor system, where LIF is used to measure the amount of CO_2 in the reactor. This has been done with technical measurements and reactivity measurements with different types of catalyst samples.

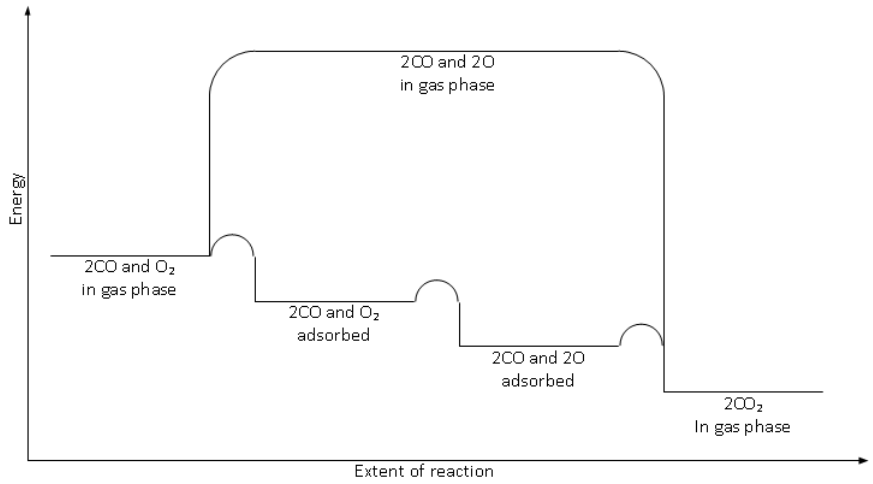

Figure 4.1: Two paths of the reaction $CO + \frac{1}{2}O_2 \rightarrow CO_2$, the energetically favorable when the molecules gets adsorbed and the energetically unfavorable in gas phase. In both of them the O_2 must dissociate.

4.1 CO Oxidation with Surface Catalysis

The CO oxidation is described by the chemical formula $CO + \frac{1}{2}O_2 \rightarrow CO_2$. For this reaction to proceed, O_2 has to dissociate into two O atoms. The dissociation almost never happens when the molecules are in gas phase because the energy needed to overcome the molecule bonds. But adsorbed at the surface of a catalytically active material this dissociation is divided into smaller steps, which all have lower barriers and are energetically favorable. In figure (4.1) a diagram of the reaction showing both the energetically unfavorable path in gas phase and the favorable adsorbed at the surface.

In the first step the molecules are adsorbed to the surface by arranging their bonds to bind also to the surface. In the second step the O_2 molecule is dissociated by losing all their internal bonds to bound to the surface only. In the third step the O finds a CO and reacts to CO_2, which will leave the surface because the filled orbitals in the molecule makes it extra stable. A more extensive explanation will be given in the LCAO model approach below.

There exist two different types of adsorption, chemisorption and physiosorbtion. Physiosorbtion is due to the weak van der Waal's force. Chemisorption is due to strong electron sharing between atoms, such as the covalent, ionic or metallic bonding. The dissociation is most probable to happen in a two steps process where the molecule first gets physiosorbed with an energy minimum further from the surface and then get chemisorbed by changing its bonds with an energy minimum lower and closer to the surface [2].

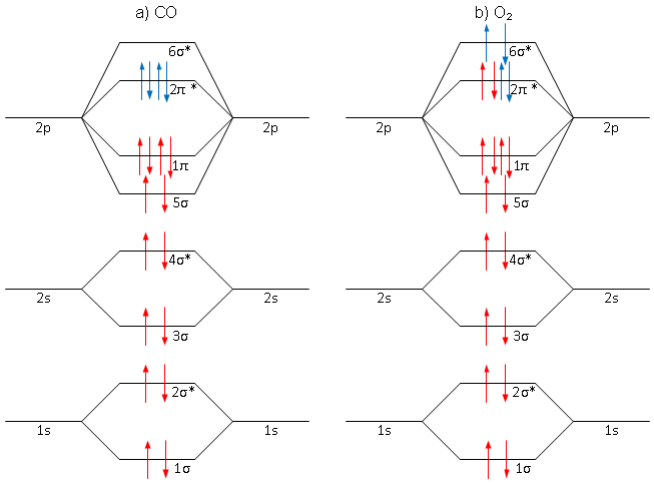

Figure 4.2: A much approximated version of the LCAO model to show the dissociation and adsorption of O_2 and CO to a catalytic active surface. In a) the orbitals are filled as for the CO molecule and in b) as for O_2. The red arrows represent electrons from the molecule and the blue from the surface. It can be seen that less electrons are needed to dissociate O_2.

4.1.1 LCAO Model Approach

When two atoms meet there will be mixing of the orbitals. The linear combination of the orbitals will describe the new molecular orbitals. This model is called LCAO (Linear Combination of Orbitals). Figure (4.2) shows a much approximated version where only those atomic orbitals with the same energy forms the new molecular orbitals. Without going into details two s atomic orbitals are giving rise to two molecular orbitals, anti-bonding σ* and bonding σ, and two p orbitals two bonding σ, π and two anti-bonding σ*,π* orbitals. In these cases, the bonding orbitals have less energy than the anti-bonding. The red arrows represent electrons in the molecule and the blue the valence electrons added from the catalytically active surface. In the case of CO and O_2 the energy of the electrons in the 1σ, $2\sigma^*$, 3σ, $4\sigma^*$ is together zero but the molecular orbitals due to the 2p are negative. The total energy sum being negative is the reason why they are molecules.

When the surface valence electrons get close to the 2p orbitals they will go over in the molecular orbital and the energy of the molecule will increase. When the molecular orbitals are filled the energy will be zero and it will be more energetically favourable for the molecule to dissociate. In the simple model O_2 needs only four electron against the 6 electrons in CO to fill the orbitals, which is the reason why only O_2 dissociates on a catalytic active surface.

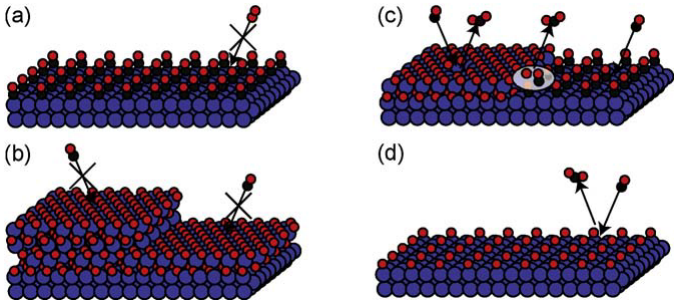

Figure 4.3: Possible oxide and adsorption phases on Rh surfaces. The surface in a) is CO poisoned, which means that no O_2 can adsorb and dissociate. The surface in b) is O poisoned, which means that no CO can adsorb on the surface. Both c) and d) are active oxygen dominated phases, where c) shows a surface oxide that is more active than the thin oxygen layer in d) according to DFT calculations. [5]

4.1.2 Different Phases at the Surface

The surface can change much during the process due to different oxides adsorbed, which of course changes the activity of the catalyst. This has been seen in several experiments, where temperature and CO/O_2 ratios have been varied [4].

In figure (4.3) are four examples of a Rh surface, where adsorbed molecules have created different phases of varying activity. In a) the surface is totally CO covered and there are no sites left for the O_2 to adsorb and dissociate and no reaction can happen, which therefore is called CO poisoning.

In b) there is a bulk oxide where all sites at the surface are occupied with O atoms and no CO can adsorb. This is therefore called oxygen poisoning.

In c) and d), two different active phases are shown. In c) the surface is partially covered with a O-Rh-O surface oxide together with metallic patches or defects where the CO can adsorb. For CO oxidation the surface oxide has been seen together with very high CO_2 production. In d) the surface is covered with dissociated oxygen. This surface makes it possible for CO to adsorb and react with O, because they do not need to dissociate. There is an ongoing debate on which of these phases is most active, but in the experiments in this project the difference between the two could not be deduced so both types are considered as one active oxygen dominated phase [6]. This example is for Rh surfaces, but similar results have been found on other metals as well, such as Pd, Ru and Pt [1].

4.2 Materials Gap

The industrial catalysts are often produced of nanoparticles dispersed in a so-called support material. The smaller the particles are the more surface per volume, which makes the total catalyst more active at lower cost. These nanoparticles consist of many different surfaces with many defects.

Traditional surface science studies uses single crystal surfaces with as little defects as possible. This means that in the models, there will be a risk to miss some of the more important properties of industrial catalysts.

The differences between the materials of the industrial catalysts and the models used in surface science are called the Materials Gap.

4.3 Pressure Gap

It has been seen that the reactivity of catalysts changes rapidly when different oxides gets adsorbed at the surface, which was described in more detail above. These oxides are often not seen at ultra high vacuum (UHV) but start to appear at higher oxygen pressures. These oxides can even be one of the main explanations to the high activity of the industrial catalysts and therefore very important to investigate. Many surface techniques demand UHV, which means that in practice these properties will be lost in the model. The difference between the pressure where the models and the industrial catalysts operates is called the Pressure Gap.

4.4 Model Catalyst Samples

When doing a model catalyst in surface science the aim is to mimic the industrial catalyst but at the same time be able to measure the surface, which of course is impossible. The approach that can be used is to compare the results from different experiments and samples going from surface techniques friendly to industrial and see the differences and similarities of them. In this project a few samples were used but only two are reported in the thesis; a more surface science friendly single crystal and a more industrial like powder sample.

4.4.1 Crystal

A crystal is a specific form of a solid where the atoms are ordered in a periodic way called lattice. The lattice will describe the total 3 dimensional crystal. One period is called a unit cell. The cell is often defined to have its edges in the middle of an atom or a group of atoms. In figure (4.4) there are three common cubic unit cells, sc (simple cubic), fcc (face centered cubic), bcc (body centered cubic) together with the sc lattice.

Surface - Miller indices: A crystal can be cut in many different ways to create different surfaces, so it is convenient to use a well-defined way to describe

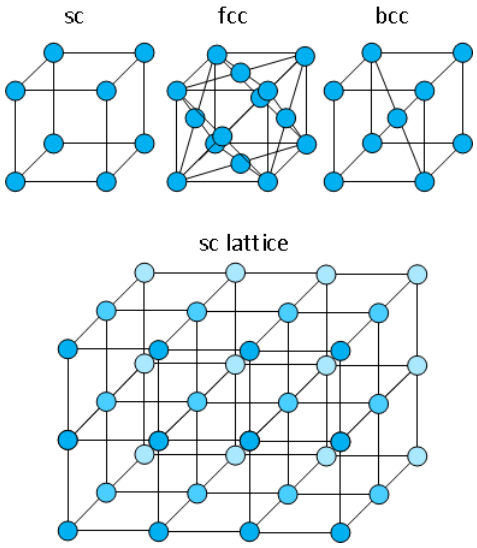

Figure 4.4: Three common cubic unit cells, sc (simple cubic), bcc (body centered cubic), fcc (face centered cubic) and the sc lattice. The blue balls represent the lattice points.

the different surfaces. Most used are the Miller indices, which describe a surface by its normal vector in the coordinates of the lattice.

If there are three axis a_1, a_2 and a_3 as in figure (4.5) then the Miller indices will be the inverse of the points where the surface plane intercepts with the lattice when the distance between the lattice points are unit along the axes. The Miller indices are often denoted as (hkl) where h, k and l are integer numbers which also describe a vector going normal to the surface according to the axis a_1, a_2 and a_3. This is maybe difficult to understand and therefore some examples are given. In figure (4.5a) is the fcc(111), which plane, lighter blue, intercepts with the axis at $(1, 1, 1)$ giving the Miller indices $(\frac{1}{1}\frac{1}{1}\frac{1}{1}) = (111)$. Orange balls represent points in the lattice that lie in the plane of the surface. In figure (4.5b) is the fcc (100), which plane intercepts with the axis at $(1, \infty, \infty)$, where infinity ∞ means that the plane will never intercept with a finite crystal, giving the Miller indices $(\frac{1}{1}\frac{1}{\infty}\frac{1}{\infty}) = (100)$. In figure (4.6) is a model of what the fcc(553) and fcc(100) look like.

4.4.2 Powder Sample

In the LIF measurement two powder samples were used, consisting of Al_2O_3 as support material impregnated with 4 % Pt and 2 % Pt + 1 % Pd respectively.

The samples are produced by first dispersing the support material in water and then adding a solution with wanted catalytic metal until desired amount has

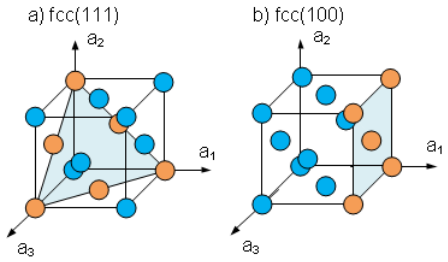

Figure 4.5: Illustration of the a) fcc(111) and b) fcc(100) with the surface represented by the brighter blue part of the figure. The orange balls are the lattice points in the surface plane. a_1, a_2 and a_3 are the axes of the cubic lattice and the distance between the lattice points are unit. In the fcc(111) the plane is intercepting with the axis at $(1,1,1)$ giving the Miller indices $(\frac{1}{1}\frac{1}{1}\frac{1}{1}) = (111)$. In the case of fcc(100) the plane intercepts with the axis at $(1,\infty,\infty)$ giving the Miller indices $(\frac{1}{1}\frac{1}{\infty}\frac{1}{\infty}) = (100)$.

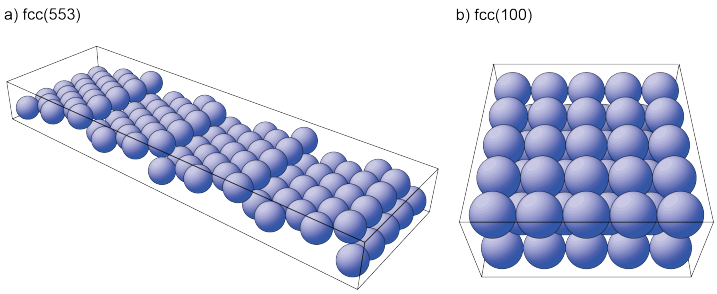

Figure 4.6: The a) $fcc(553)$ and b) $fcc(100)$ surfaces. [9]

been reached. The mixture is finally freeze dried by first cooling it with liquid nitrogen and calcined by slowly increasing the temperature to about 500°C. The resulting sample will have many facets and defects that will increase the activity.

4.4.3 The Sample Reactivity

The atoms form crystals because it is energetically favourable to share the electrons between each other to get more filled orbitals. At the surface of a crystal the atoms will have less neighbouring atoms and therefore less filled orbitals, which gives higher energy. This is easiest to understand with a simplified example. In the fcc structure every atom in the bulk will have 12 nearest neighbours. The fcc(100) surface atoms will have 4 less neighbours as compared to an atom in the bulk and therefore be less stable.

In a simple but rather good approximation one can say that more neighbours give a less reactive atom. A surface of a material with more defects (kinks, steps, holes and so on) will therefore be more reactive than the same surface with no defects. For example the high indices surface in figure (4.6a) will be more reactive than the low indices surface in figure (4.6b) and therefore also the first step to better mimic an industrial catalyst. Because of the same reason a powder sample, described above, will also be more reactive than a single crystal surface sample.

4.5 This Project

In this project, we use a new type of reactor that uses LIF to measure the amount of CO_2 produced in CO or CH_4 oxidation just above the sample. The different parts of the reactor will be described and the reasons for building it like that. The setup was tested in a more technical aspect and different proposals on improvements will be presented.

Also two reactivity measurements will be presented. The first experiment with Pd(100) and PdAg(100) surfaces using only the QMS, aiming at understanding the overall process of these catalysts and see the difference between the two samples because of the possible segregating Pd atoms in the alloy to the surface creating an equally active sample as the Pd only.

The second was to measure the activity of two very good catalytic powder samples, where LIF was used to measure the CO_2 concentration in the reactor. The aim was to compare the different results of the samples but also general aspects of catalyst will be presented.

These two experiments are also a kind of reference for the performance of the system.

5 The Reactor System

This part will describe the technical aspect of the construction, the performance at the end of the project and possible improvements of the system. This will be presented in three different sections, specification, performance and improvements.

5.1 Specification

The system should be used to measure the produced CO_2 in CO and CH_4 oxidation on catalysts in a reactor with LIF. In an experiment the amount of gases should also be followed with a Qudrupole Mass Spectrometer (QMS). The temperature should be controllable and measurable too.

For the LIF measurements, two CaF windows are used to let the exciting laser light in and out of the reactor. The fluorescence is measured with an Infrared (IR) camera through a third window perpendicular to the laser sheet. The reactor cell needs to be large enough such that more than one sample can be used at the same time for comparison between them. The windows need to be in the size of the cell such that the outgoing fluorescence light gives a spatial resolution of the CO_2 in the reactor.

The system should be able to do both batch and flow experiment, such that the samples properties can be followed against temperature (flow), pressure and gas composition (batch). These three properties must also be measureable at the same time as the LIF measurement.

The experiments should be done with many different pressures and gas ratios from low to more industrial like atmospheric pressures. The pressure must therefore be determined with quite good accuracy. To be effective it must be easy to change the gas mixture in the reactor within a minimum of time.

The systems material must be catalytically inactive so the system itself does not influence the process of gas and sample. It is good if the system can be constructed in as many ways as possible, such that it can be rebuilt to be as effective as possible for a specific measurement and for new parts to be attached. To be able to measure different samples during short time the sample holder particularly should be easy to remove and reattach.

5.2 Design

This section will describe the different parts of the system with considerations taken into account when constructing it. Figure (5.1) is a picture of the set up used during a LIF experiment and figure (5.2) an overview of the system with arrows describing the path of the gas when it is used in flow mode.

The laser light is going into the reactor through the window behind and out through the window in front of the reactor, according to the picture. In the reactor, some of the laser light is exciting the CO_2 molecules and the light emitted from the molecules is measured with the IR camera through the window perpendicular to the laser sheet. Trough two openings in the top flange gas is

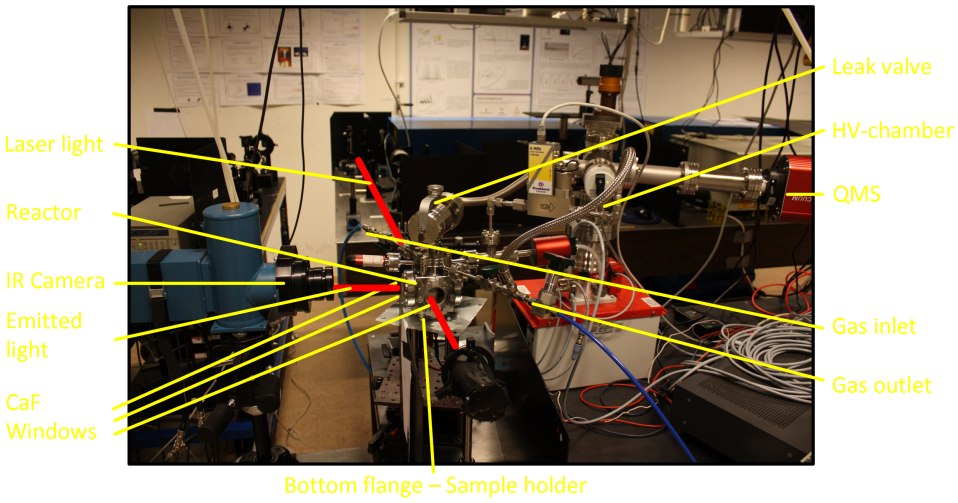

Figure 5.1: Picture of the set up used during a LIF measurement.

pumped through the reactor with the gas system (not shown in the picture). In the top flange a leak valve is also attached for letting a small amount of the gas into the high vacuum (HV) chamber for gas analysis with the QMS. The sample holder is attached to the bottom flange.

5.2.1 Gas System

A schematic drawing of the gas system is found in figure (5.3). It consist of five Bronkhorst EL-FLOW flow controllers [11] that can let 1-50 mln/min (1 mln = 1 ml at standard (normal) pressure and temperature) of a certain gas through each controller and one Bronkhorst EL-PRESS pressure controller [11] that can control the pressure in the reactor between about 0 - 1000 mbar. The direction of the gas flow is controlled by five electronic valves, ten manual screw valves [13] and five manual mechanical valves.

There is a possibility to choose gas mixture from five different gases, more if there already is a gas mixture in the bottles, with the ratio between 2 % / 98 % to 50 % / 50 % for two gases. The pressure controller makes it possible to do flow measurement with a specific pressure in the reactor and the valves and the pressure controller closest to the reactor can be closed for experiments in batch mode. The Bronkhorst controllers are computer controlled enabling remolty changing of gases. The gas system is also mobile and easy to attach which makes it possible to use with other systems than the specific system described in this thesis.

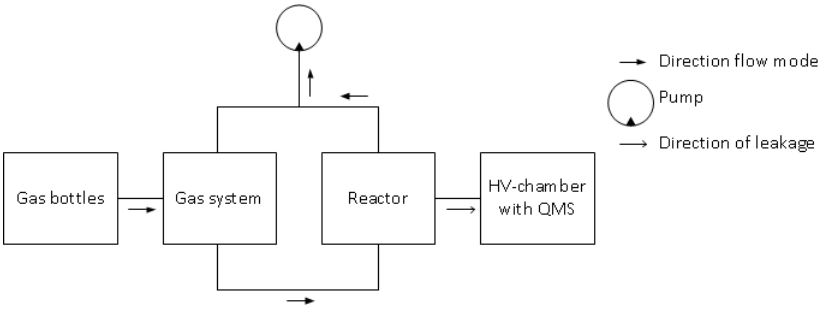

Figure 5.2: A schematic view of the system. The central part is the reactor. From the gas bottles different gas mixtures, selected with the gas system, are pumped through the system. The reactor also has a leakage valve that lets gas into a HV-chamber for mass analysis with the attached QMS.

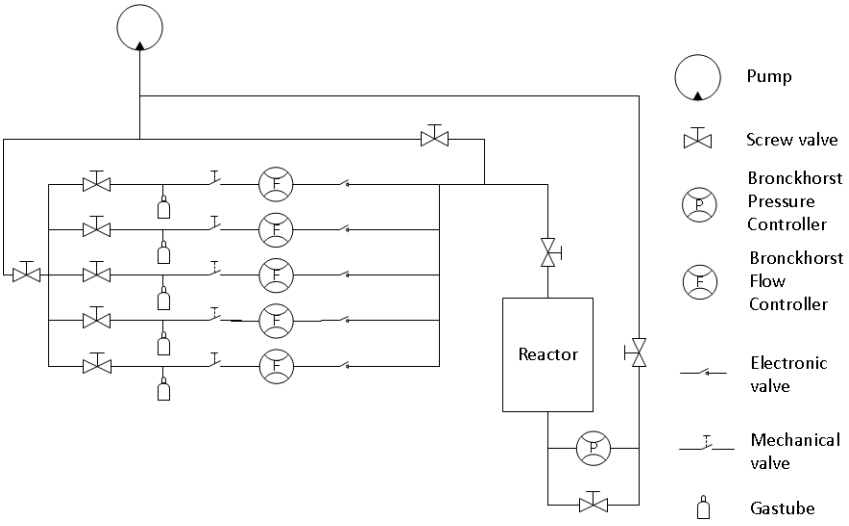

Figure 5.3: A schematic drawing of the gas system. It consists of different valves controlling the direction of the gas pumped through the system. Five flow controllers decides the composition of gas into the system. The pressure in the reactor is controlled with a pressure controller.

5.2.2 Quadrupole Mass Spectrometer - Theory

The QMS is widely used instead of traditional mass spectrometers for chemical analysis. The main difference between the two is that the traditional mass spectrometer disperses the ions in space or time while the QMS filters out the molecules according to the created ions mass to charge m/e ratio. By letting the QMS filter out different masses, with the difference of < 1 amu between the masses, it can be continuously used as a spectrometer and that is why it is often called QMS. It is not as good as the traditional mass spectrometers when it comes to resolving and performing precise mass measurements, but there are several advantages with this device. It is very simple and small because it does not have magnets that are expensive, heavy and mechanically slow to move. It filters the ions on the basis of mass and charge which is good when measuring ions with many different velocities. The mass selection of the QMS is changed electronically, instead of mechanically as for the traditional mass spectrometer, which makes it good for experiments where one needs to change the resolution remotely [7].

The main parts of a QMS are Ion source, Quadrupole Mass Filter (QMF) and detector. These parts are connected to each other such that ions can be steered through the system with electric fields. An individual description of the parts will be given below.

Ion Source: The ion source main parts are a cathode and an anode creating an electric field between them. The cathode is heated to start emitting electrons that will accelerate towards the anode. Gas molecules leaked into the QMS will be positively ionized by the electrons. The molecules will in the interaction with the electrons also get different kinetic energies and the resulting ions will be affected by the electric field, which means that they can hit each other producing more types of ions. Example of different types of ions due to the occurrences in the ion source is $ABC^{+}+2e^{-}$, $ABC^{3+}+3e^{-}$, $AB^{+}+C+2e^{-}$, $BC^{+}+A+2e^{-}$, where A,B and C are parts of molecule ABC [7]. Each kind of molecules will therefore get its own set of ions, cracking pattern, which can be used to distinguish between different types of gases.

Quadrupole Mass Filter (QMF): The QMF consists of four parallel electrodes with the ends forming a square as in figure (5.4). Two of the rods are connected to the mostly negative part and two are connected to the mostly positive part of a bias which consists of both a DC and AC voltage. Between the rods there will be an electrical quadrupole field.

The path of different ions, through the QMF will be affected by the alternating voltage and their mass to charge ratio m/e.

If the DC part is zero, the effect on the ions will be equal from alternating positive and negative voltage. Positive ions will therefore be accelerated towards the electrode when the voltage is negative and towards the centre axis when the electrode is positive. If the ion m/e ratio is low enough or the time the electrodes

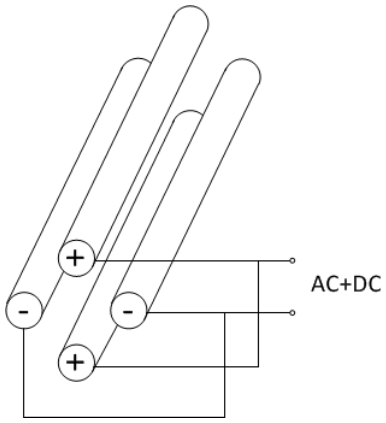

Figure 5.4: Sketch of the electrodes in the QMF. They are connected to a bias as in the figure. The AC amplitude is set to a higher value then the DC voltage making the total voltage on the rods to oscillate in time with different long time as positive and negative. The plus and minus sign on the rods represent the sign of the voltage most of the time. By choosing a specific AC and DC voltage, only ions with a certain mass to charge m/e ratio are allowed to pass the filter.

are negative is long enough it will hit one of the electrodes, discharge and not pass through the filter [10].

By adding the DC part the total voltage oscillation will be around another position than zero. The two electrodes with positive DC voltage will have longer time with positive voltage and shorter time with negative voltage, if the amplitude of the AC voltage is higher than the DC voltage. In this situation ions with high m/e ratio will not have the time to accelerate before the AC voltage changes sign and therefore stay in the middle of the quadrupole field and the two electrodes. These two electrodes will therefore only allow ions with high enough m/e ratio to pass the filter [10].

The other two electrodes will have the same DC but with changed sign and the AC voltage half a period off relative the other two more positive electrodes. They will not allow the ions with low m/e ratio to pass the filter, because they do not have time to accelerate during the short time of negative voltage.

The voltage can be set to act as a band pass filter for the ions only allowing one m/e ratio to pass [10]. In figure (5.5) the paths of three different ions are illustrated. In a) is the path of an ion with too low m/e ratio, in b) is the m/e ratio too high and in c) the same ratio as the one that are allowed too pass.

Detector: Both ions with too high or too low mass to charge ratio will be discharged against one of the electrodes and only the ions with mass allowed to pass will hit the detector. The detector in the QMS we used consists of both a

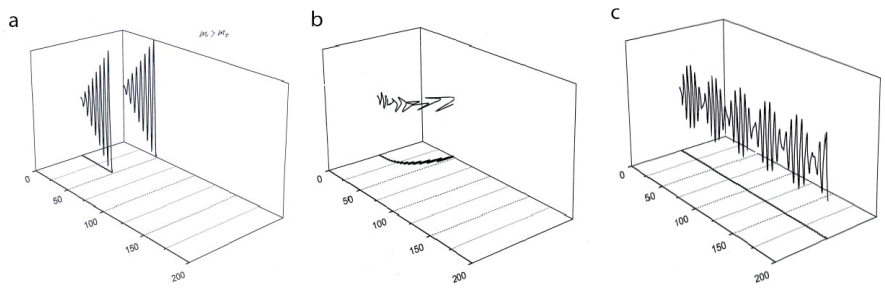

Figure 5.5: Plot of the paths of three different ions through the filter. Figure a) ions with lower mass to charge m/e ratio than the allowed to pass, b) ions with higher mass to charge m/e ratio than the allowed to pass and c) ions with the same mass to charge m/e ratio as the allowed to pass. Both the ions in a) and b) will be discharged against the electrodes and not pass to the detector. [8]

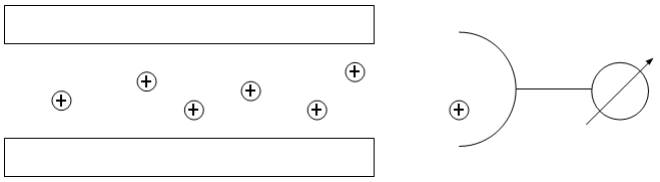

Figure 5.6: Drawing of the Faraday cup. The ions (positive circles) that pass the QMF will hit the cup (half circle) and change the charge of the cup. The change of charge is then measured.

Faraday Cup and a Continuous Secondary Electrons Multiplier (C-SEM). The Faraday cup is used to measure large ion current but cannot resolve smaller currents. The C-SEM on the other hand uses a system that can resolve even small ion currents. Due to the angle with which the ions are going into the two detectors, both of them can be attached at the same time [7].

Faraday Cup: Figure (5.6) is a drawing of the Faraday cup. The ions, (rings with a plus signs), that pass the electrodes will hit the cup, (half circle), and change the charge of the cup. The change in charge which is proportional to the total charge of all ions hitting the cup is then measured [7].

The Faraday cup has a very simple, robust design and is tolerant against high temperatures, which makes it possible to use for long time without calibration. The big disadvantage with this device is that it is not good for small ion currents [7].

Continuous-Secondary Electron Multiplier (C-SEM): Figure (5.7) is a drawing of the C-SEM. It consists of a glass tube and a conversion dynode

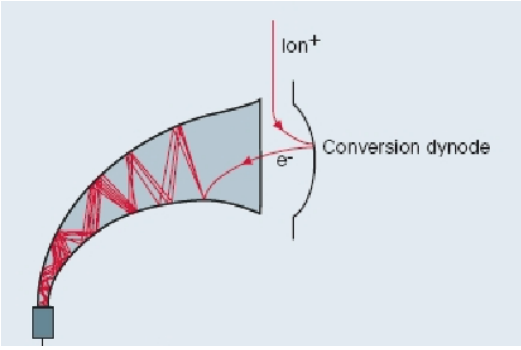

Figure 5.7: Drawing of the C-SEM. It consists of a glass tube with the inside coated and a conversion dynode consisting of a conductive material that have high resistance and low work function. This material will emit electrons when hit by ions or electrons [7]. A high voltage applied gives an electric field to steer the electron forward in the tube. The electrons hit the walls of the tube many times creating an avalanche of electrons that can be measured at the end of the tube. [7]

with the inside covered with a conductive material that has high resistance and low work function. It will emit electrons when ion or electron impact [7]. The tube is connected to a high voltage that creates an electric field, which steers the electrons not only just to hit the walls of the tube but also forward in the tube. The electrons will travel along the glass tube and hit the walls of the tube several times creating an avalanche of electrons that is measured at the end.

There are two advantages of a C-SEM over a Faraday cup. The C-SEM can measure much smaller ion currents and because of that it does not need as much gas to measure at a specific m/e ratio, which lower the measuring time.

5.2.3 Quadrupole Mass Spectrometer - Setup

Figure (5.8) is a schematic view of the HV-chamber with a Pfeiffer vacuum QMA 200 PTM25252 [12] QMS attached. The central part is the HV-chamber, needed because of the low pressure the QMS must operate in. The HV-Chamber is filled with a small amount of gas from the reactor through a leak valve. The QMS is connected to a computer through the data collector unit QME 220 PTM28611 [12], which continuously plots the selected mass to charge ratios as an ion current. The HV-chamber is connected to a Pfeiffer vacuum Hi Pace 80 turbo pump [12] to evacuating the HV-chamber to the region around 10^{-8} mbar. The leakage is set to get up the pressure to 10^{-6} mbar where the QMS operates best. The pump can also be used to evacuate the reactor if connected directly to the HV-chamber creating high vacuum in the reactor making it possible to use standard surface technique preparations.

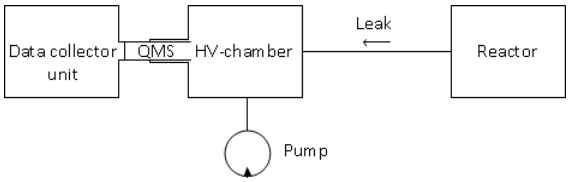

Figure 5.8: Schematic view of the QMS. It consists of a HV-chamber pumped with a turbo pump. The QMS is attached to the side of the reactor. When measuring, a small amount of gas is leaked with a leak valve from the reactor into the HV-chamber.

5.2.4 Reactor

Figure (5.9) shows a schematic view of the reactor with different measuring devices attached to it. It consists of a cube with six stainless steel flanges attached to the sides. Three of them have CaF windows, which let infrared laser light through. One of the flanges has four pipes to be used for inlet and outlet of gas and connection of pressure gauges. In the figure this flange is connected to the top of the cube but it can also be attached to any other side. At the top there is also a pipe that lets a small amount of the gas into the HV-chamber controlled by a sensitive screw leak valve. This makes it possible to set the pressure very accurately to about 5×10^{-6} mbar in the HV-chamber. There are two different Pfeiffer Vacuum pressure gauges attached, CMR 361, for pressure measurement between 1×10^{-1} mbar and 1100 mbar of all gases and TPR 280, for pressure measurement between $5 \times 10^{-4} - 1000$ mbar for air, O_2, CO and N_2. The Sample holder is attached in the bottom flange in the picture but it can also be attach to other sides if the sample is fixed at the holder, as described in next section. The reactor can also be directly attached to the HV-chamber to use the better turbo pump to get pressures in the reactor where standard surface preparation techniques can be used.

5.2.5 Sample Holder

Figure (5.10) is an illustration of the sample holder. All the parts are chosen not to be catalytically active and to avoid nickel that can create carbonyls, which can adsorb everywhere and interfere with the experiment. The holder is attached to the flange through two Tantalum metallic rods that are glued to the flange. The sample is heated with a bias, controlled through the rods, over a bohr electric heater that are attached to the holder. To measure the temperature a type C thermocouple (tungsten 95% rhenium 5% - tungsten 74% rhenium 26%) is used for temperature measurements between 0 - 2320 °C [3]. For best result the thermocouple should be spot welded to the side of the sample but to weld it to any metallic parts in direct contact with the sample is often good enough. Welding it to the sample holder makes it easier to switch between samples, which can be a big advantage. The flange with the holder is attached

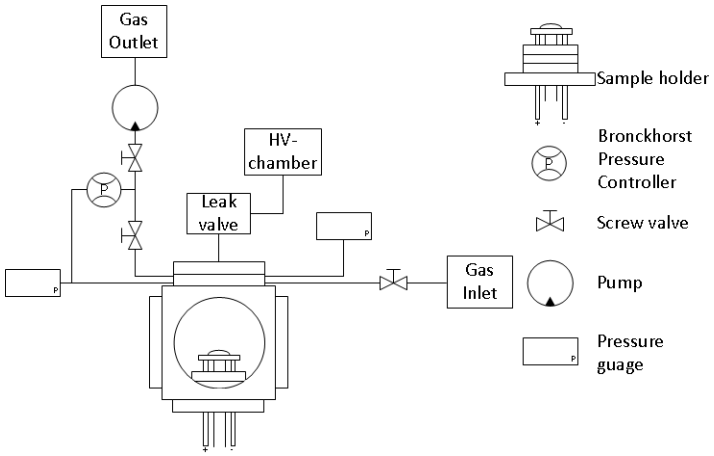

Figure 5.9: Overview of the reactor with different devices attached. The reactor consists of a cube with six stainless steel flanges attached to the sides. From one of the flanges the sample holder is attached, in the figure from the bottom. In one of the flanges, the top in the figure, four pipes are welded to the side for attaching points for inlet, outlet, and the two different pressure gauges. There are also CaF windows in three of the flanges that allow infrared light to pass.

to the reactor cube as an individual part and can therefore easily be removed in order to change sample etc.

In the LIF measurement the sample plate material was Molybdenum, due to its high resistance against heat and oxidation in oxygen rich environments. Other sample holders can also be used that for example can hold ordinary crystal samples with a sort of clips. This kind was used in the Pd experiments.

5.3 Performance

The basic performance of the system has been tested at less accurate experiments, which will describe the system in a more technical aspect. Other parts of the report will describe experiments where the system has been used, which in one way also are testing the performance, maybe even better.

5.3.1 Gas System

The gas system could pump the reactor down to 10^{-2} mbar in the best, depending on how much the reactor is leaking.

The time to fill the chamber is specified in table (5.1). It was measured by letting 50 mln/min of air pass through the Bronkhorst flow controller (calibrated for NO but differing with 3 % only if used for air). The time was manually read from a stopwatch, the flow from the Bronkhorst flow controller and the pressure from the CMR 361 gauge, which do not give accurate results but the main

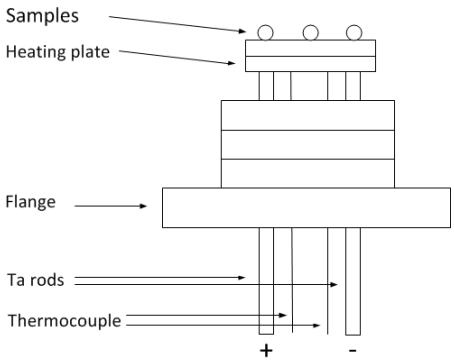

Figure 5.10: Drawing of the sample holder. It consists of two Tantalum metallic rods, glued to a flange, where the holder is attached. The heating of the sample is controlled through the rods by applying a bias to each of them. The thin lines represent the type C thermocouple wires attached either to the sample or any material in direct contact with the sample.

properties. It can be seen that the flow is constant, 50 mln/min, before getting significantly lowered at about 900 mbar, which means that the flow controller does not have the capacity to keep the flow at these high pressures.

Three different ways to evacuate the system were measured: The first by using only the pressure controller, the second using both the pressure controller and the screw valve after the outlet of the reactor and the third using only the screw valve at the inlet, all with the starting pressure 1000 mbar. The result is presented in table (5.2). It shows that the best way is to use the screw valve at the outlet of the reactor. Using both the outlet valve and the Bronkhorst Pressure controller did not decrease the time much but lowered the minimum pressure slightly. There are also the opportunity to pump the reactor from all openings but this should not give a significantly quicker dumping but after long time give the possible minimum pressure of 10^{-2} mbar.

To be able to control the gas composition in a flow experiement, the gas should be changed as quickly as possible. To get a clue about the time one experiment was done, in which the reactor was first filled to 1000 mbar of air and then was the gas exchanged by flowing O_2 instead. The time it took for the mass 32 signal, mostly O_2, to go from being stable for totally air filled to totally O_2 filled reactor will then be extracted. The result is plotted in figure (5.11) and the time between the black vertical lines, for which the signal is considered stable, is almost one hour. This means that to keep a stable gas mixture during an experiment is very difficult, if not impossible. The time of course will be better if the reactor is held at lower pressure and the gas flow is maximized.

Pressure(mbar)	Time(m:s)	Flow(mln/min)
10^{-2}	0:00	50
100	0:25	50
200	0:48	50
300	1:13	50
400	1:38	50
500	2:02	50
600	2:26	50
700	2:51	49.87
800	3:15	49.70
900	3:41	47.00
1000	4:23	1.80

Table 5.1: Time to fill the chamber to a certain pressure. The flow is constant to about 900 mbar.

Opening	End pressure (mbar)	Time(m:s)
Bronkhorst Pressure controller	5	1:22
Screw valve outlet	2	0:25
Bronkhorst Pressure controller + Screw valve outlet	1.5	0.43
Screw valve inlet	10	2:44

Table 5.2: Time to pump the system of the reactor measured with the pressure gauges. It can be seen that the best way is to open the screw valve at the outlet.

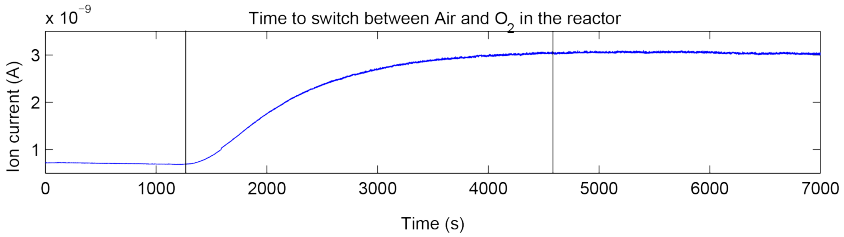

Figure 5.11: Time to totally change the gas composition in the reactor. Starting with 1000 mbar of air and then by flowing 50 mln/min of O_2 totally change the composition. The time between when mass 32 signal, plotted in the figure, is stable in the totally air environment and totally O_2 environment was considered to be about one hour between the black vertical lines.

5.3.2 QMS

The QMS is attached to the system as a complete unit and therefore not tested here. The performance in this section will more test the properties of how the gases travel to the QMS.

The long pipe between the HV-chamber and the reactor introduces a time delay between the real reaction and the measured with the QMS. This time delay was measured by taking the difference at a point where the activity is changing much in the LIF signal, where the change can be seen directly, and the QMS signal. In figure (5.12a) the CO_2 signal from the QMS (red) is plotted together with the LIF signal (black) and b) is a zoomed part of a). The temperature that, like the LIF signal, directly reacts on a change in activity, is plotted as blue. If looking at about $t = 300$ s the change of activity in the QMS signal is only a few seconds after the LIF signal, but the QMS gets much more smeared out than the LIF signal. This is for example a problem if looking at the LIF signal at $t = 400$ s where the activity rapidly goes up again but because of the smearing it will be harder to see in the QMS signal. This is bad for example if comparing two or more samples that become active at different pressures or temperatures.

5.3.3 Reactor

The volume of the reactor together with the part of the pipes from the reactor to the closest valves was measured to be about 200 ml. This was done by measuring the time, t, it takes to fill the reactor to 500 mbar (half full) with a constant flow rate $f = 50$ mln/min. The full volume is then given by $V = 2tf$. The reactor is larger than normally used for catalyst studies.

5.3.4 Sample Holder

The time to replace the sample can be less than 15 min if it does not need to be fixed or the thermocouple wire needs to be welded to the sample again.

In a CH_4 oxidation experiment it was formed some kind of oxide with the Molybdenum holder at high temperature, about 650 °C. This coincided with a lower activity and therefore probably had an impact on the catalytic reactions.

5.4 Improvements

This section will include proposals on things that can be improved, which have been seen in the performance and the reactivity measurements with the system.

5.4.1 Gas System

In the first batch experiments the Bronkhorst controller was used to set the pressure in the reactor, which took some time before it was stabilized. During this stabilizing process and during the filling the reaction did already start,

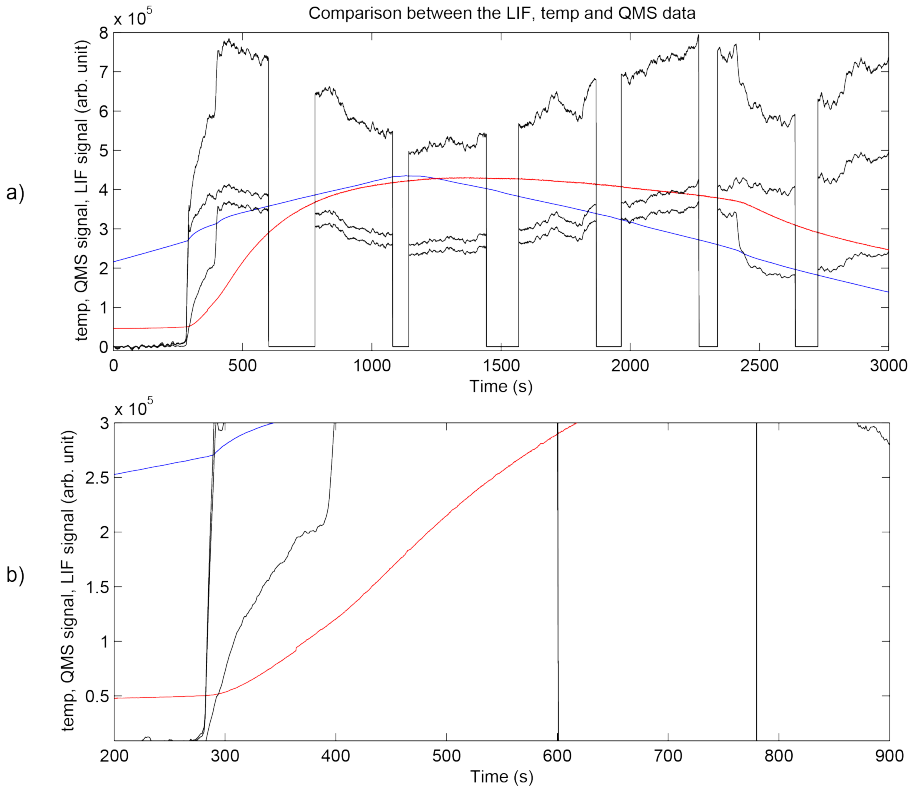

Figure 5.12: Comparison of the LIF (black) and QMS (red) signal for CO_2. In a) the whole test is displayed and in b) a zoomed part of the beginning. It can be seen that the QMS almost directly notices the change in the reaction rate, but it is much more smeared out. The temperature (blue) is also plotted.

which made it difficult to know the correct gas composition when the reactor finally was batched. To get better control of this the time between the start of the filling and the start of the batch should be as short as possible. One solution is to just stop the filling at the proper pressure in the reactor instead of using the pressure controller. This was done manually in later batch experiments but with difficulties to correctly set the wanted pressure. To avoid this manual error the flow could be stopped automatically at a certain time when the desired pressure is reached. As the system is now, this can be implemented at the electronic valves but it would be better if the flow was stopped closer to the reactor, which can be done by changing the screw valve against an electronic valve.

Now experiments are done more manually, changing the direction of the flow, temperature etc. This implies that all experiments will have slightly different starting values. By automating the controls, these differences and the time needed to control the experiment could be minimized and more accurate.

5.4.2 Reactor

The reactor inlet and outlet of gas is done from the same flange, either at the top or the bottom of the reactor. The shortest path for the incoming gas is to flow along the flange to the outlet without passing the sample. A solution can be to have the inlet in the bottom flange and the outlet in the top flange, or vice versa, 180° from each other. The shortest way for the gas to flow from the inlet to the outlet is then through the middle of the reactor where the sample is placed. Another solution is to have the inlet and outlet in the middle of the bottom and top flange, which maybe is better but more complicated to implement. It could also be better to have two inlets and two outlets, which should change the gas in the reactor quicker, but the question is if the new gas will go directly to the nearest outlet and not pass by the sample. The disadvantage with all these solutions is that one more part has to be removed when changing samples.

To measure the effects of different inlets and outlets, one can use the LIF. By first sending in an amount of non-reacting gas, such as Argon, and then switch to CO_2, the path of the CO_2 in the reactor can be monitored.

When doing the LIF measurement it was difficult to change samples, because the whole reactor was attached through the sample holder. A thinkable solution is to only attach the whole reactor in the top flange. Then, the bottom flange with sample holder could easily be removed without having to remove any other parts.

5.4.3 Sample Holder

Now the temperature is changed manually by changing the current through the bohr electric heater, which means that the temperature will be changed for different pressures due to less amount of gas for the heat to transfer away from the sample. If a PID controller (adjusting the heating current, using the difference between the wanted temperature and the measured temperature from the thermocouple) was used, the temperature could be held practically constant

during a switch of gases and also during a whole experiment. This would also make it possible to avoid that the exothermic effect of the oxidation changes the temperature and influences the experiment.

The sample plate used in the LIF measurement has to be changed to a more heat and O_2 resistant material for CH_4 oxidation experiments, which need high temperatures in order to get a noticeable activity. One solution can be to use some kind of ceramic plate that absolutely not creates oxides. Another solution is to use some kind of heat resistant paint that will stop the gas from getting in contact with the Molybdenum.

6 Reactivity measurements

After the characterization of the system, a few reactivity measurements were done, in order to investigate the properties of some model catalysts. The results also provide some further information on the performance of the system.

6.1 CO Oxidation of Pd(100) and $Pd_{75}Ag_{25}$(100)

The aim of this experiment was to investigate the effect of mixing Pd with Ag. It has been seen in other experiments that an oxide is positively affecting CO oxidation. This oxide is also more energetically favourable and for the crystal to lower its energy the Pd atoms in the alloy should segregate up to the surface to form a stronger oxide and an active catalyst.

6.1.1 Experiment

The CO oxidation experiments over Pd(100) and $Pd_{75}Ag_{25}$(100) were done in batch mode with starting pressure 600 mbar for different CO/O_2 ratios. During the experiment the gas mixture and sample temperature were monitored. Since each O_2 can oxidize two CO molecules, the environment will get more and more oxidizing. Hence, the different activity phases at different CO/O_2 ratios will be seen in the same experiment.

6.1.2 Results and Discussion

Figure (6.1) and (6.2) show the results from two experiments on Pd(100) with starting conditions of 308 mbar CO, 292 mbar O_2 at 350°C and 200 mbar CO, 400 mbar O_2 at 300°C respectively. Figure (6.3) shows corresponding results from the $Pd_{75}Ag_{25}$(100) surface with starting conditions of 225 mbar CO, 375 mbar O_2 at 350°C. Panel a) shows the QMS signal for the gases involved in the CO oxidation, panel b) the CO/O_2 ratio and panel c) the CO_2 production. Since every O_2 molecule can oxidize two CO molecules, the CO/O_2 ratio drops as the reaction runs. Before $t = 0$ the gas mixture was filling the reactor to a pressure of 600 mbar and at $t = 0$, short after the batching of the reactor, the pressure was stable.

Starting with figure (6.1); from the beginning, until the first black line the CO_2 production is low since the surface is CO poisoned. After the first black line, when the CO/O_2 ratio has decreased, the CO_2 production rapidly increases due to oxygen replacing CO as the dominating adsorbate on the surface. When the production peaks, the MTL (Mass Transfer Limit) is reached, which means that it is not the reactivity of the surface that stops the increase of production but instead the amount of CO that reaches the surface. In the third phase, the CO_2 production drops slowly as the CO partial pressure decreases.

In figure (6.2) and (6.3) the same three phases can be seen, but with some slight differences. In figure (6.1) and (6.3) there is some activity already in the first phase, although the CO/O_2 ratio is higher, which should lead to more CO

poisoning. The reason is that the temperature is higher, which increases the CO desorption rate and lifts the CO poisoning.

Looking at the increase of the production in the second phase it is steeper in the pure Pd samples, figure (6.1) and (6.2), than in the alloy, figure (6.3). The explanation can be that the surface of the alloy has less Pd atoms in the beginning. As the surface is exposed to oxygen, however, the Pd atoms start to segregate such that in the end the surface will be almost full of Pd atoms, and as good a catalyst as the pure Pd samples. This is seen in the production peaks that are almost at the same height in all three experiments.

The production peak in figure (6.1) is slightly higher than in the other two. Probably the oxide is equally good in both the experiments on pure Pd, but the amount of CO left when reaching the peak in the CO_2 production is different and the activity will not be the same.

6.1.3 Conclusion

In the experiment three different production phases are seen on all experiments similar to what has been seen in previous other experiments. There was a slight difference in the activity of the phases between the different surfaces, but the different temperatures and CO/O_2 ratios can be the explanation for that.

In the case of the $Pd_{75}Ag_{25}(100)$ surface the increase of CO_2 production was slower, but almost the same production peak was finally reached. The explanation can be that it takes time for the Pd atoms to segregate to the surface but when it is full with Pd atoms it will be almost equal to the surface of the pure Pd samples.

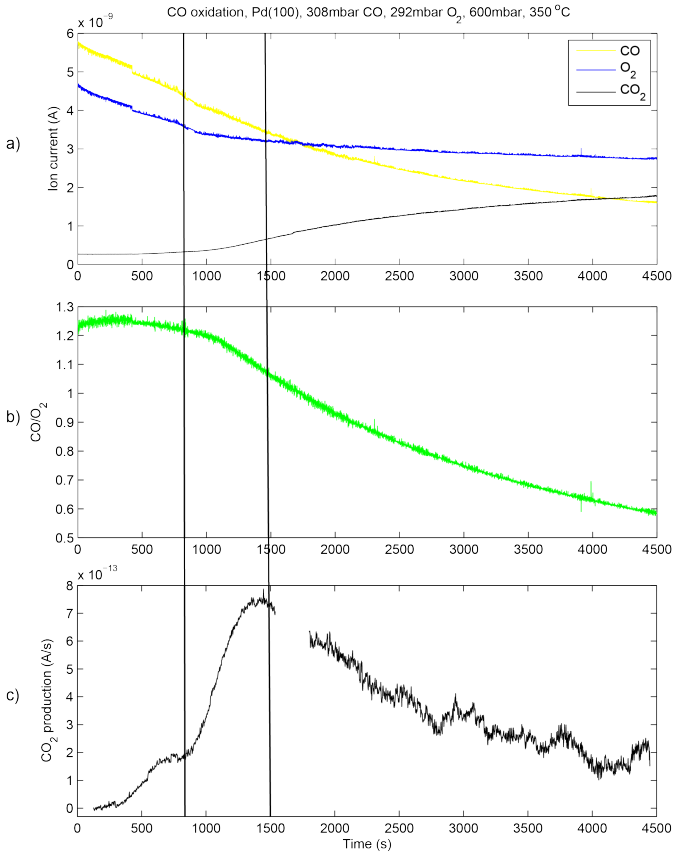

Figure 6.1: CO oxidation of Pd(100) with starting pressure 308 mbar CO and 292 mbar O_2 in batch mode at 350°C. The gas sample is first mixed outside the reactor and then allowed to fill the reactor to 600 mbar. At $t = 0$ as soon as a pressure of 600 mbar was reached, the reactor was batched. Since CO oxidation uses two CO for every O_2, the CO/O_2 ratio will decrease and create a more oxidizing environment for the surface. This is monitored in b) and is the only significant change of experimental conditions in the batch experiments. Looking at the CO_2 production curve three phases can be seen, first from $t \approx 0$ to $t \approx 900$ s, second from $t \approx 900$ s to $t \approx 1300$ s and third from $t \approx 1300$ s to $t \approx 4500$ s.

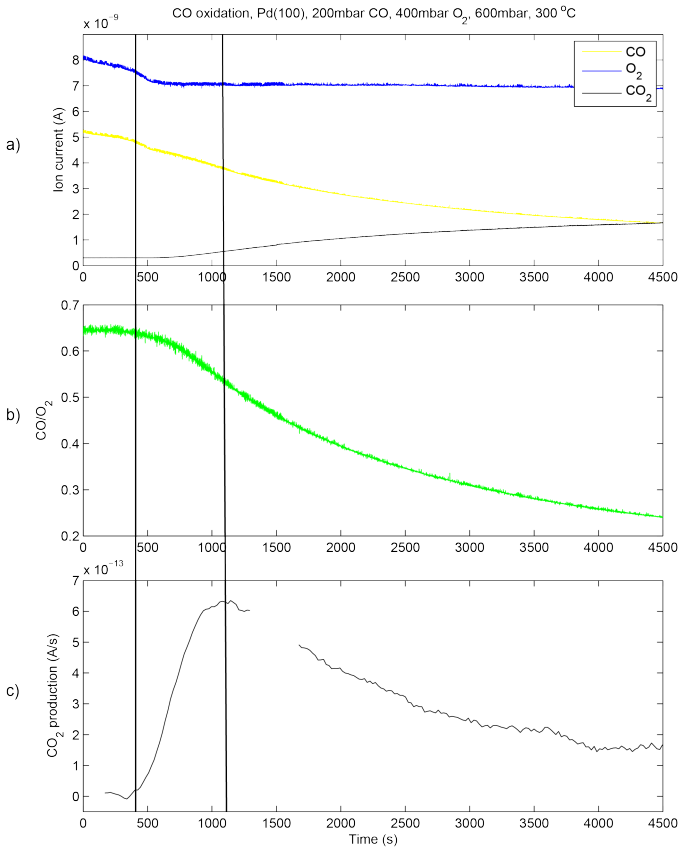

Figure 6.2: CO oxidation of Pd(100) with starting pressure 200 mbar CO and 400 mbar O_2 in batch mode at 300°C. The gas sample is first mixed outside the reactor and then allowed to fill the reactor to 600 mbar. At $t = 0$ as soon as a pressure of 600 mbar was reached, the reactor was batched. Since CO oxidation uses two CO for every O_2, the CO/O_2 ratio decrease creating a more oxidizing environment for the surface. This is monitored in b) and is the only significant change of experimental conditions in the batch experiments. Looking at the CO_2 production curve three phases can be seen, first from $t \approx 0$ to $t \approx 400$ s, second from $t \approx 400$ s to $t \approx 1200$ s and third from $t \approx 1200$ s to $t \approx 4500$ s.

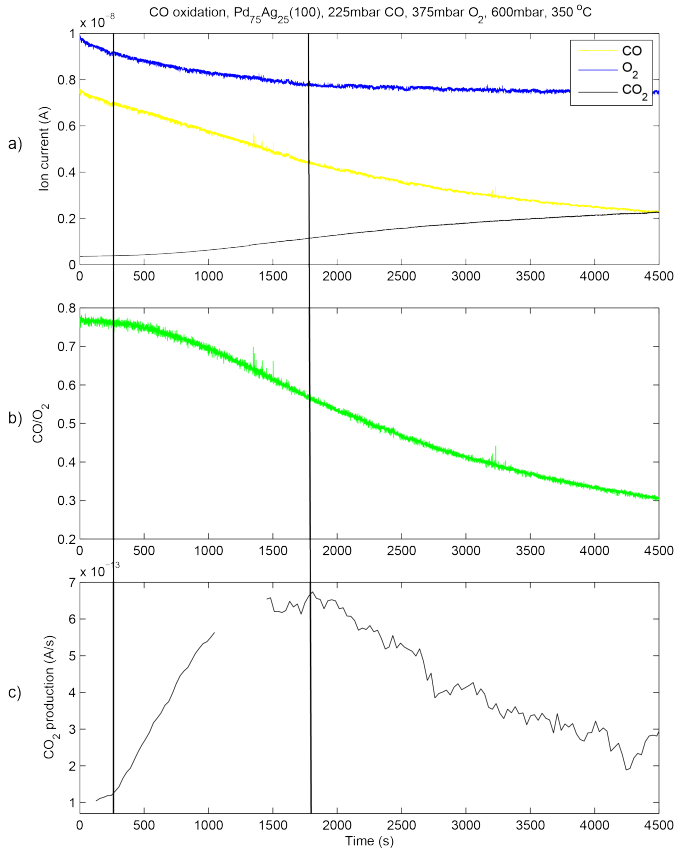

Figure 6.3: CO oxidation of $Pd_{75}Ag_{25}(100)$ with starting pressure 225 mbar CO and 375 mbar O_2 in batch mode at 350°C. The gas sample is first mixed outside the reactor and then allowed to fill the reactor to 600 mbar. At $t = 0$ as soon as a pressure of 600 mbar was reached, the reactor was batched. Since CO oxidation uses two CO for every O_2, the CO/O_2 ratio will decrease and create a more oxidizing environment for the surface. This is monitored in b) and is the only significant change of experimental conditions in the batch experiments. Looking at the CO_2 production curve three phases can be seen, first from $t \approx 0$ and $t \approx 250$ s, second from $t \approx 250$ s to $t \approx 1400$ s and third from $t \approx 1400$ s to $t \approx 4500$ s.

6.2 LIF as a Tool to Monitor Catalytic Reactions

The primary aim of the experiment was to investigate the system in a technical aspect and which properties that can be seen.

6.2.1 Experiment

In this experiment we used two Al_2O_3 pellet samples impregnated with 4 % Pt and 2 % Pt + 1 % Pd respectively. The experiment was done in flow mode with a constant pressure and a constant incoming gas mixture, while the temperature was ramped up and down. During the experiment the gas composition and sample temperature were monitored as above. In an addition, the CO_2 concentration above the samples were measured using LIF. The experiment was done in such a way, so that the different phases of activity of the sample could be seen in the same experiment for both samples.

6.2.2 Results and Discussion

Figure (6.4) shows the result from the experiment. In d) five snapshot taken by the IR camera are displayed, monitoring the fluorescence at times when the CO_2 production changed rapidly. Panel a) shows the intensity in the left half (4 % Pt, blue line), the right half (2 % Pt + 1% Pd, black line) and the whole (red line) of the snapshots taken continuously by the IR camera. Panel b) shows the temperature and panel c) the QMS CO_2 ion current. The yellow vertical lines shows when the CO_2 production of the samples changes rapidly.

Before the experiment started, the gas system was set to flow 20 mln/min O_2, 30 mln/min CO and the pressure in the reactor to be constant at 200 mbar. The LIF measurement started at $t = 0$.

It can be seen that the intensity is almost zero until the right sample (2 % Pt + 1 % Pd) starts to be active at the first yellow line and the left sample (4 % Pt) starts to be active at the second yellow line. This can also be seen in the three first snapshots and in the temperature. Before the samples get active the surface of them are CO poisoned but as the temperature increases the CO desorption rate also increases, and the CO poisoning is gradually lifted.

The increase of the heating proceeds until $t \approx 1200$ s where it instead is decreased and at the third yellow line the left sample is inactive again, which also can be seen in snapshot four. The right sample continues to be active even after the heating is off and first when the oxygen flow was reduced, first to 15 mln/min at $t \approx 4700$ s and then 10 mln/min at $t \approx 4900$ s it gets inactive, which can also be seen in snapshot five.

It is very clear that the right sample (2 % Pt + 1 % Pd) gets active at a lower temperature than the left sample. This indicates that the Pd atoms are less sensitive to CO poisoning than the Pt atoms, because the CO poisoning gets lifted at lower temperature for the sample with Pd.

The exothermic effect of the reaction can be seen as the temperature more rapidly increases when the sample starts to be active. Another way to look at it is plotted in figure (6.5), which shows the ion current against the heating current

and the measured temperature against the heating current in panel a) and b) respectively. The plots starts at heating current 0.8 A and at 1 A, the right sample is active, seen in both a) and b), and at slightly higher current the left sample is also active, easiest to see in b). Then the heating current is increased to 1.35 A and then decreased again, but as can be seen the exothermic effect is keeping an elevated sample temperature and also because of that the activity of the sample stays. At heating current 0.65 A the left sample is deactivated, seen in both the plots as rapid changes.

To do a better comparison between the two the signal from the IR camera could be used to measure the sample temperature, but because of several effects that has not been taken account while doing the measurement, this was not possible.

Overall it turn out that these samples are much more active than single crystal samples because of much more surface area.

In a more technical aspect it is in a) and d) very clear when the samples start and finish to be active. This also shows that it is possible to do a live comparison between the two samples in the reactor.

6.2.3 Conclusion

The experiment showed that the 2 % Pt + 1% Pd sample goes into the active phase at lower temperature than the 4 % Pt sample. The explanation can be that the Pd atoms are less sensitive to CO poisoning.

In the experiment many interesting things could be seen, such as the exothermic affect which also is more prominent in the 2 % Pt + 1% Pd case.

The more important conclusion from this test is that the system worked as it was meant. With the LIF it is possible to see the different activity phases very clear and the two samples could be compared live in the same experiment.

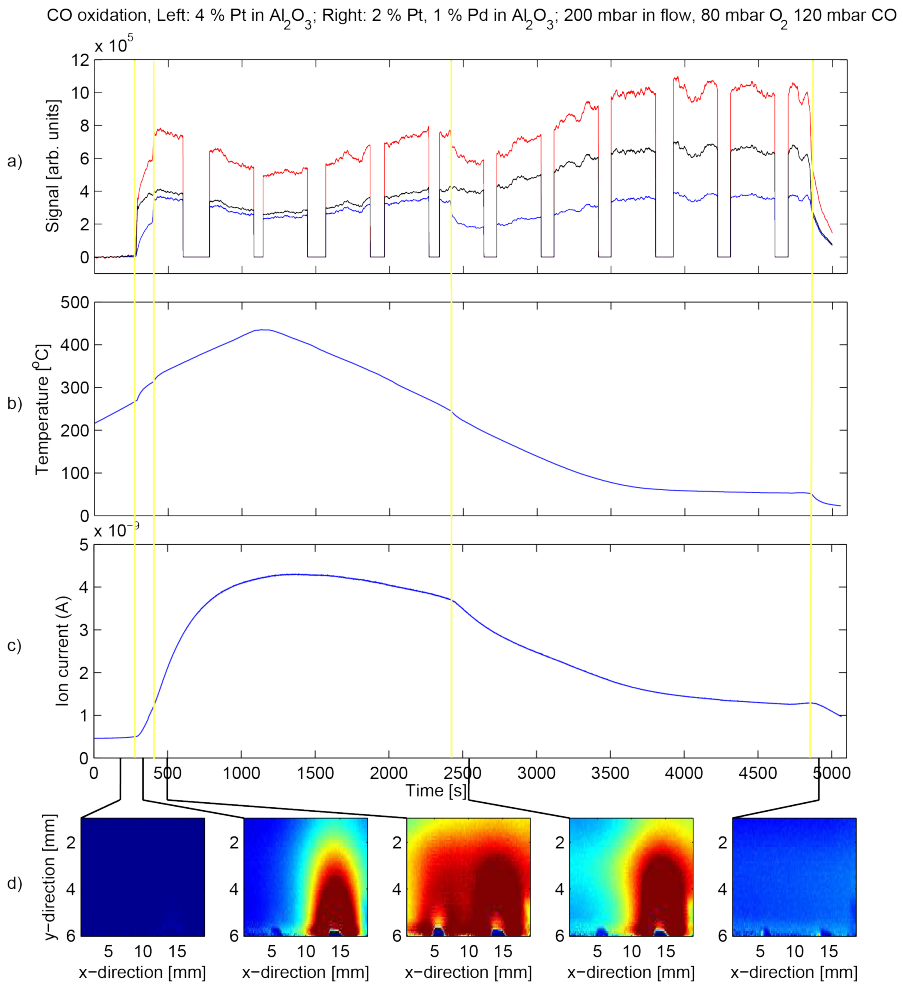

Figure 6.4: The result from the measurement of the powder samples using LIF. In d) five snapshots are taken by the IR camera at times when the activity of the samples changed rapidly. In panel a) the intensity in the area the same as the snapshot is summed and plotted as red colour. The blue line represents the total intensity over the left half of the area showing the activity of the 4 % Pt sample and the black line shows the total intensity over the right half showing the intensity over the 2 % Pt + 1 % Pd sample. Panel b) shows the temperature and panel c) the CO_2 ion current from the QMS. The yellow vertical lines shows when the CO_2 production of the samples changes rapidly.

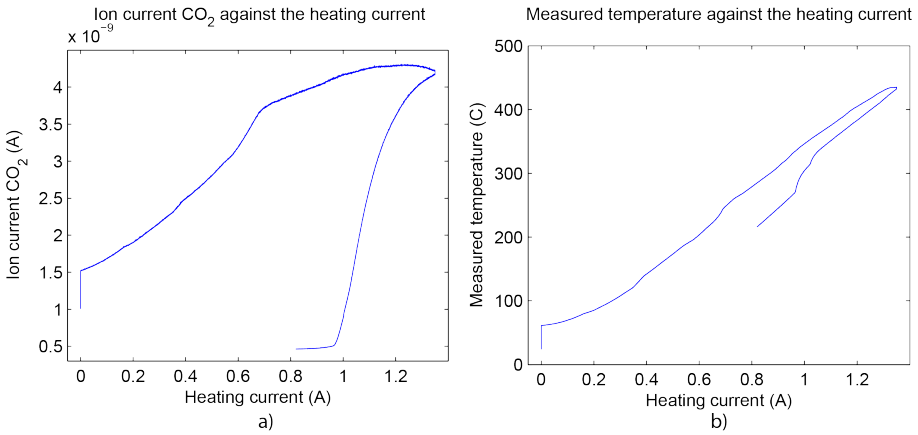

Figure 6.5: Two plots showing the exothermic effect. Panel a) shows the ion current of CO_2 against the heating current and b) the measured temperature against the heating current. The experiment started at heating current 0.8 A. It can be seen that the production in a) and measured temperature in b) is higher when the current is decreased then when it is increased. This shows that the catalyst heats it self and needs less external heating when it is active.

7 Summary

The aim of the project was to characterize an oxidation reactor system that could measure the amount of CO_2 with LIF. The performance of the system was measured in a technical aspect to understand the shortcomings and benefits of the system. Also different types of reactivity experiments were done, two which is reported in this thesis.

The resulting system consists of a gas system, a reactor with sample holder and a HV-chamber for QMS analysis.

The reactivity measurements on Pd(100) and $Pd_{75}Ag_{25}(100)$ were done in batch mode and the CO_2 production was followed with the QMS. The results show that both types of samples had two clear phases: one active and one inactive depending on the CO/O_2 ratio. For the alloy, the time before reaching the maximum CO_2 production was longer, but the peak was as high as for the pure Pd samples. The explanation can be that it takes some time for the Pd atoms to segregate to the surface but when it has, the activity will be as for the pure Pd sample.

In the other reactivity measurement, LIF was used to measure the CO_2 production over two different powder samples with Pt or a mixture of Pd and Pt as the active material. There was a clear difference in the temperature where the CO poisoning was lifted, which was straight forward to follow with LIF.

In a technical manner this test was successfully showing that the idea of the system worked. It was clear to see the different activity phases for the two samples and the differences could also be seen in the same experiment. With some improvements, future measurement can give more accurate results and the future of the system seems to be good. The next step is to use less reactive samples and study CH_4 oxidation.

References

[1] J.W.M. Frenken B.L.M. Hendriksen, S.C. Bobaru. Oscillatory co oxidation on pd(1 0 0) studied with in situ scanning tunneling microscopy. *Surf. Sci.*, 552:229–242, 2004.

[2] Michael Bowker. *The Basis and Application of Heterogenous Catalysis.* Oxford Science Publications, 1998.

[3] en.wikipedia.org/wiki/Thermocouple. Wikipedia thermocouple. 2010-04-19.

[4] J. Gustafson et al. Sensity of catalysis to surface structure: The example of co oxidation on rh under realistic conditions. *Physical Reviev B.*

[5] J. Gustafson et al. Structure and catalytic reactivity of rh oxides. *Catalysis Today*, 145:227–235, 2009.

[6] R Westerström et al. Structure and reactivity of a model catalyst alloy under realistic conditions. *J. Phys.: Condens. Matter*, 20, 2008.

[7] http://www.pfeiffer-vacuum.com/know-how/mass-spectrometers-and-residual-gas-analysis/introduction-operating-principle/quadrupole-mass-spectrometers-qms/ion sources/technology.action?chapter=tec4.1.2.2. Pfeiffer vacuum. 2011-03-04.

[8] http://www.qmg700.com/quadinfo/Literature/Quadrupole Pdf. 2011-06-14.

[9] Fritz Rammer Klaus Hermann. Surface explorer. http://surfexp.fhi-berlin.mpg.de/, 2011-04-20.

[10] Philip E. Miller and M. Bonner Denton. The quadrupole mass filter: Basic operation concepts. *Chemical Education*, 63:617–623, 1986.

[11] www.bronkhorst.com. Bronkhorst. 2011-04-19.

[12] www.pfeiffer vacuum.com. Pfeiffer vacuum. 2011-04-19.

[13] www.swagelok.com. Swagelok. 2011-04-19.